Journal of Alloys and Compounds 480 (2009) 662–665

Contents lists available at ScienceDirect

Journal of Alloys and Compounds

journal homepage: www.elsevier.com/locate/jallcom

Strengthening mechanism of SiC-particulate reinforced Sn–3.7Ag–0.9Zn lead-free solder

X. Wang, Y.C. Liu*, C. Wei, H.X. Gao, P. Jiang, L.M. Yu

School of Materials Science & Engineering, Tianjin Key Laboratory of Advanced Jointing Technology, Tianjin University, Tianjin 300072, PR China

ARTICLE INFO

Article history:
Received 17 December 2008
Received in revised form 24 January 2009
Accepted 1 February 2009
Available online 10 February 2009

Keywords:
Lead-free solder
Composites
Microstructure
Microhardness

ABSTRACT

Mechanically mixing was adopted to prepare SiC-particulate reinforced Sn–3.7Ag–0.9Zn composite solders and the effects of SiC addition on the solidification behavior, melting behavior and the corresponding microhardness of air-cooled composite solders were explored. It is found that the addition of SiC particles into the Sn–3.7Ag–0.9Zn alloy melt prompts the formation of primary β-Sn phase in the solidified structure. For the SiC particles serve as additional nucleation sites for the formation of primary β-Sn phase, the sizes of both the β-Sn dendrites and the intermetallic compounds (IMCs) decrease gradually with the SiC particles increasing. The hard SiC particles and refined β-Sn dendrites and IMCs could obstruct the dislocation slipping and thus lead to a strong strengthening effect in the composite solder.

© 2009 Elsevier B.V. All rights reserved.

1. Introduction

The Sn–Pb solder is widely applied in the electronic packaging due to its good performance. In recent years, the lead-containing solder was prohibited to use by legal laws and regulations for the reason that Pb is harmful [1]. Since the solder would bear most of mechanical, electrical and thermal load in service, high joint reliability is urgently requested as the rapid development of modern micro-electronic industries [2].

Binary or ternary Sn-base lead-free alloys are currently taken as the replacements of Pb–Sn solder [3]. Among them the Sn–Ag system is the most promising substitute, due to its superior ductility, creep resistance and thermal resistance [4,5]. Continuous effort to bring the third even the fourth component, such as Cu [6], In [7], Bi [8], Zn [9] and so on, into the Sn–Ag system has been made to obtain the high performance. It was recognized that the addition of Zn to the Sn–Ag alloy could decrease its melting point and improve its mechanical strength, creep resistance and thermal fatigue resistance [9,7]. Furthermore, the addition of Zn made the Sn–Ag solder get a better oxidation resistance due to the formation of Ag–Zn intermetallic compounds (IMCs) [10]. Hence, the Sn–Ag–Zn solder is promising for the further development of the lead-free solders.

Except for that, attempts of adding reinforcing particles to form composite solders were made. Shen et al. [11] investigated the Sn–3.5Ag–ZrO_2 composite solders and found that the size of primary β-Sn dendrites and IMCs was refined. Tai et al. [12] studied the performance of nano-Ag-reinforced Sn–0.7Cu composite solder and found an improved wettability, mechanical property and creep fracture cycle. Liu et al. [13] explored the effect of nano-SiC addition on microstructure and microhardness of Sn–Ag–Cu solder and made similar conclusion as in Ref. [11]. Additionally, Nai et al. [14] and Mohan Kumar et al. [15] tried to strengthen the Sn–Ag–Cu solders by the addition of multiwalled carbon nanotubes and single-wall carbon nanotubes, respectively.

Since various reinforcing particles were proved to be effective surface active reagents and the thus prepared composite solders exhibit improved mechanical performance. Attempts for introducing SiC particles into the Sn–3.7Ag–0.9Zn eutectic alloy were made first here by means of mechanical mixing. The effects of SiC additions on the solidified structure, melting behavior and microhardness of the eutectic solder are also investigated. Furthermore, the corresponding strengthening mechanisms of the SiC-reinforced composite solder are discussed considering both the microstructural observation and hardness measurement.

2. Experimental procedures

The Sn–3.7Ag–0.9Zn eutectic solders (in mass) were prepared from bulk Sn, Ag and Zn rods (all with a purity of 4 N). The process of melting was carried out in a vacuum arc furnace under the protection of a high purity argon atmosphere at 400 °C for about 30 min. In order to get a homogeneous composition within the ingots, the alloy was remelted five times to produce button-like specimen with a diameter of about 3.5 cm. Finally it was casted in a water-cooled copper mould.

The composite solder was prepared by mechanically mixing SiC particles (with an average size of 1 μm) into the Sn–3.7Sn–0.9Zn alloy melt. During preparation, the pre-weighted ingot and SiC particles were first put into an Al_2O_3 crucible and then was heated up to 250 °C. After that, an electromagnetic stirrer was activated to

* Corresponding author. Tel.: +86 22 87401873; fax: +86 22 87401873.
E-mail address: licmtju@163.com (Y.C. Liu).

0925-8388/$ – see front matter © 2009 Elsevier B.V. All rights reserved.
doi:10.1016/j.jallcom.2009.02.002

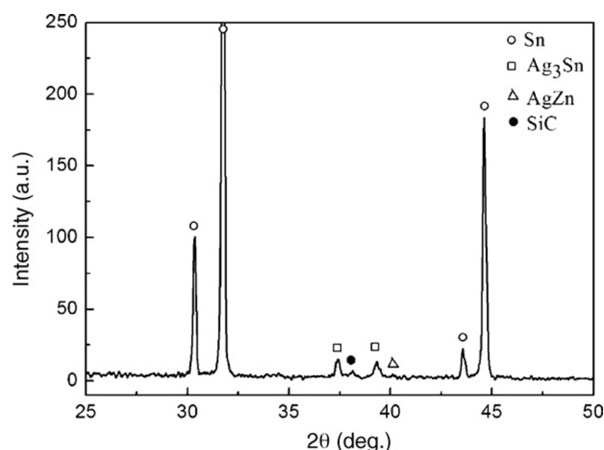

Fig. 1. X-ray diffraction pattern of the Sn–3.7Ag–0.9Zn-0.1SiC composite solder.

mechanically mix the SiC particles into the melt for 30 min to ensure a homogeneous distribution of the reinforcing particles.

Standard metallographic procedures were adopted to observe the solidified microstructures of the explored solders. The specimens were first polished and then etched with a solution of 5 vol.% HNO_3 + 95 vol.% C_2H_5OH. Scanning electron microscopy (XL30ESEM and JSM-6700F) was used to explore the structural features. Energy diffraction spectrometer and X-ray diffraction were adopted to identify the phase structure of the prepared composite solder.

A Netzsch DSC 404C apparatus was used for the measurement of the melting temperature. During it, the specimen was first heated up to 270 °C and kept at this temperature for 10 min. Then it was cooled down to room temperature at a rate of 5 °C/min.

An MH-6 hardness tester (with a tip angle of 136°) was adopted for the measurement of the hardness. The corresponding values for Vickers hardness were obtained as:

$$H_v = 1.854\frac{F}{d^2}$$

where F is the applied load and d is the average length of diagonals. The applied load and loading period are 10 g and 5 s, respectively. For each sample, 10 random points were measured and the arithmetical mean values were evaluated as the final hardness.

3. Result and discussion

3.1. Phase determination of the composite solders

The existence of SiC particles in the composite solder has to be testified first. Fig. 1 illustrates the X-ray diffraction spectrum of the prepared Sn–3.7Ag–0.9Zn–0.1SiC composite solder. As seen from it, the prepared composite solder is mainly composed of β-Sn phase, IMCs of Ag_3Sn and AgZn. Due to the minor addition of the SiC particles, there is only a small peak identified as SiC in the measured XRD spectrum. Further TEM observation and EDX analysis was also

Table 1
Elemental percentages of the region (a), as illustrated in Fig. 2, in the microstructure of the Sn–3.7Ag–0.9Zn–0.1SiC composite solder.

Elements	wt.%
Sn L	75.1
Si K	17.2
C K	7.7

performed to verify the existence of SiC particles within the solidified solder. Fig. 2 shows the SiC particles (region a) distributing within the microstructure of the composite solder (the corresponding EDX analysis results gathered in Table 1). It has to be pointed that tin was also detected in region a for the existence of Sn around the reinforcing SiC particle.

3.2. Roles of SiC addition on the microstructural formation

According to Ref. [16], the microstructure of the Sn–3.7Ag–0.9Zn solder is composed of the primary β-Sn phase and mixed granules of Ag_3Sn and AgZn IMCs which is homogeneously dispersed in the β-Sn matrix (see Fig. 3). After mechanically mixing with the reinforcing SiC particles into the eutectic solder, there are so many primary β-Sn dendrites formed in the explored Sn–3.7Ag–0.9Zn–xSiC (x = 0.05 and 0.1) composite solders (see Fig. 3b and c), and the sizes of the primary β-Sn dendrites and the IMCs decrease with increasing the amount of the SiC particles. Note that most IMCs of Ag_3Sn and AgZn accumulate at the grain boundaries of the β-Sn dendrites (see Fig. 4), which could be taken as the product phases after the formation of the β-Sn phase.

According to the theory of heterogeneous nucleation, the primary β-Sn phase could nucleate adherent to surface of the reinforcing SiC particles, which first favor the formation of the β-Sn phase, and the thus formed primary β-Sn phases would again serve as the nucleation substrates for the IMCs. Hence, the corresponding size of the β-Sn phase and IMCs decreases in the solidified microstructure of the composite solder as the increase of the SiC addtions.

3.3. Melting behaviors

Fig. 5 represents the measured DSC curves of the investigated solders. For each solder, only one eutectic peak is observed and the melting temperatures of the explored composites are lower than that of the eutectic alloy. It is also found that the melting point of the composite solder decreases with the increase of the amount of SiC particles. The decrease in the melting point of the composite solders could be possibly attributed to an increase of the surface instability and the variation in physical properties of the grain boundary/interfacial characteristics rendered by the reinforcing SiC particles.

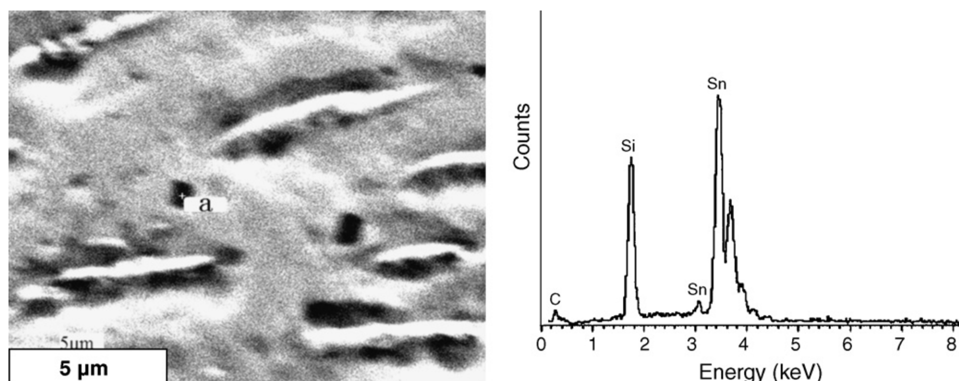

Fig. 2. EDX analysis result of the region (a) in the Sn–3.7Ag–0.9Zn–0.1SiC composite solder.

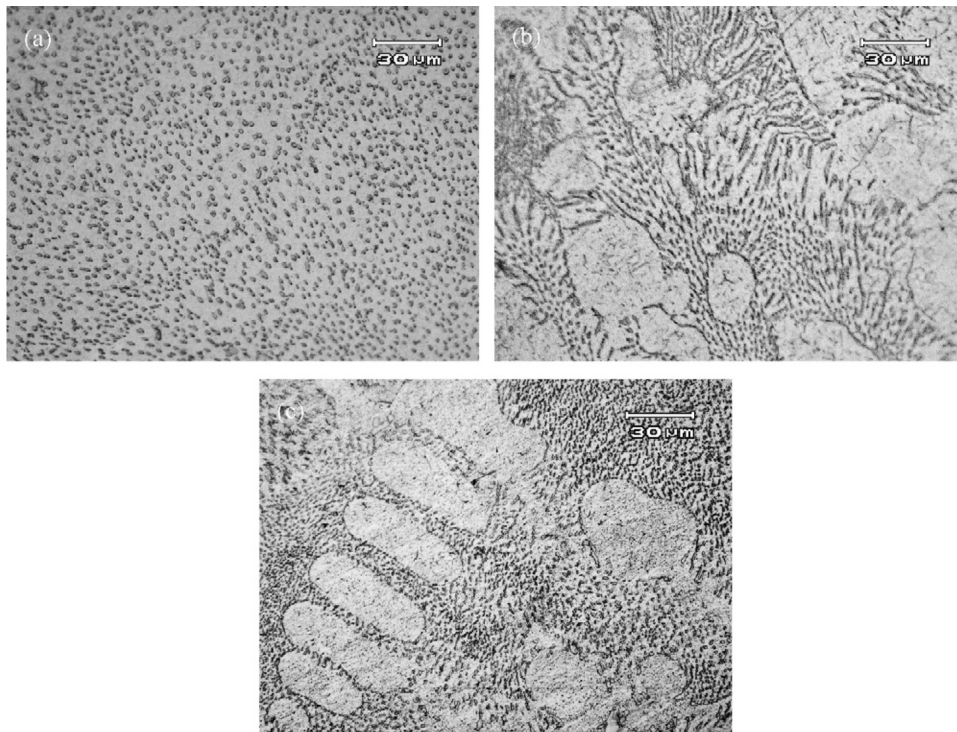

Fig. 3. Optical images of the Sn–3.7Ag–0.9Zn–*x*SiC composite solders, (a) $x = 0$, (b) $x = 0.05$ and (c) $x = 0.1$.

3.4. Microhardness measurements

Hardness measurement offers useful guidance of the mechanical performance, and the corresponding value provides an indication of resistance to deformation, densification, and cracking. The thus obtained values for hardness of the explored composite solders are collected in Fig. 6. As seen from it, the microhardness value of the composite solders increases first with the increase of the amount of SiC.

3.5. Strengthening mechanism of the SiC-reinforced composite solders

As observed from the microstructural observation, the reinforcing SiC particles, the refined β-Sn dendrites and the IMCs of Ag_3Sn and AgZn could be attributed as the main reasons for the improved microhardness of the Sn–Ag–Zn composite solders. Hence, the strengthening mechanism of the explored Sn–3.7Ag–0.9Zn–*x*SiC ($x = 0$, 0.05 and 0.1) composite solders could be explained by the plastic deformation behavior in the stressed material:

(i) The hard SiC particles distributing within the β-Sn matrix act as the pinning centers for the movement of dislocations, which correspond to a dispersion strengthening mechanism. The dislocations cannot pass through hard SiC particles, only bypass them when applied certain stress.
(ii) The refined grain boundaries obstruct the motion of dislocations, and thus lead to a dislocation accumulation at the grain boundaries. The pass of plastic deformation among the β-Sn dendrites requires more energy and the grain boundary prevents further slip of the dislocations in the case of low shearing stress. Note that there are some dislocations produced from the identical sources (for example, the pinning SiC particles) and possess the same slipping plane and orientation. These type of dislocation would accumulate around the boundaries of the β-Sn dendrites and repel the successive ones with the same sign. Thus, massive slipping of dislocation is blocked by the grain boundaries, which corresponds to a strengthening mechanism of refined grains.
(iii) The homogeneously dispersed IMCs of Ag_3Sn and AgZn at the grain boundaries of the β-Sn dendrites prevent the slipping of dislocations and thus lead to an additional secondary strengthening effect in the explored Sn–Ag–Zn composite solder.

The strengthening mechanism discussed above could be adopted to explain the effects of SiC addition on the measured hardness values. For the composite solders with 0.05 wt.% and 0.1 wt.% SiC, the grain refinement of the β-Sn dendrites, the dispersion of SiC particles and the secondary IMCs play a role of strengthening, which reflects the slight increase of the measured hardness as the SiC addition (see Fig. 6).

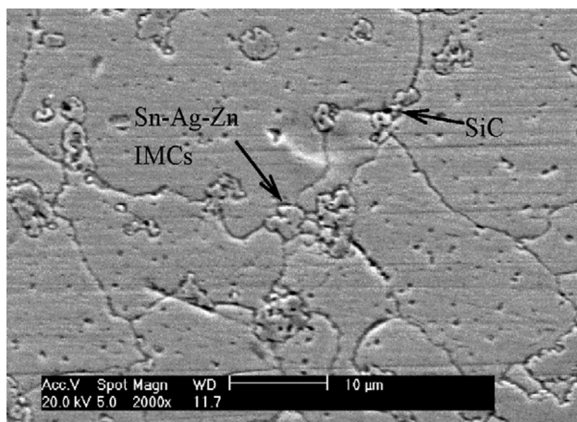

Fig. 4. SEM micrograph of the SiC-reinforced Sn–3.7Ag–0.9Zn composite solder.

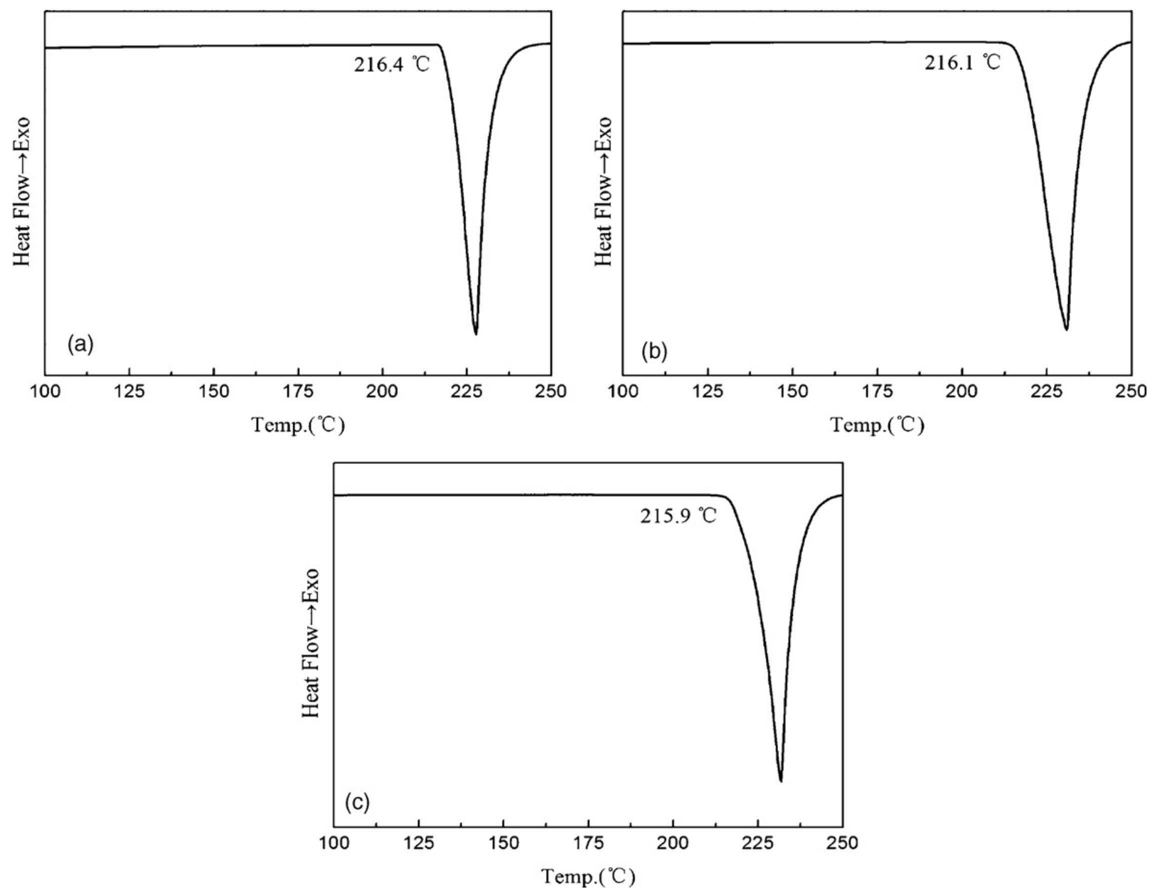

Fig. 5. DSC curves of the Sn–3.7Ag–0.9Zn–xSiC composite solders, (a) $x = 0$, (b) $x = 0.05$ and (c) $x = 0.1$.

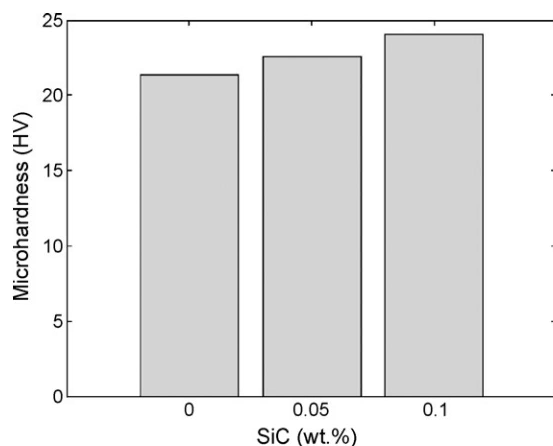

Fig. 6. Measured microhardness values of the Sn–3.7Ag–0.9Zn–xSiC ($x = 0$, 0.05 and 0.1) composite solders.

4. Conclusions

For the addition of reinforcing SiC particles in Sn–3.7Ag–0.9Zn eutectic solder provides addition nucleation sites and reduced the surface energy of the β-Sn phase, primary β-Sn dendrites formed before the onset of eutectic reaction in the composite solder. The size of the β-Sn dendrites and the IMCs decreases as the content of SiC increases from 0.05 wt.% to 0.1 wt.%.

The melting temperature of the composite solders was found to be lower than that of the eutectic alloy. The increase tendency of the measured microhardness of composite solders could be attributed to effects of grain refinement, dispersion strengthening and secondary strengthening mechanisms.

Acknowledgements

The authors are grateful to the Natural Science Foundation of Tianjin City (no.07JCZDJC01200), the Keygrant Project of Chinese Ministry of Education (no. 707012), the National Natural Science Foundation of China and Shanghai Baosteel Group Company (no. 50834011) for grant and financial support.

References

[1] M. Abtew, G. Selvaduray, Mater. Sci. Eng. R27 (2000) 95–141.
[2] K.J.R. Wassink, M.M.F. Verguld, Manufacturing Techniques for Surface Mounted Assemblies, Electrochemical Publications Ltd., 1995, p. 17.
[3] K. Zeng, K.N. Tu, Mater. Sci. Eng. R38 (2002) 55–105.
[4] L. Huang, Q. Wang, J.S. Ma, Proceedings of International Symposium on Electronic Materials and Packaging, 2000, pp. 191–193.
[5] F. Ochoa, J.J. Williams, N. Chawla, J. Electron. Mater. 32 (2003) 1414–1420.
[6] M.L. Huang, L. Wang, Metal. Mater. Trans. A 36 (2005) 1439–1446.
[7] W.K. Choi, J.H. Kim, S.W. Jeong, et al., J. Mater. Res. 17 (2002) 43–51.
[8] M. He, V.L. Acoff, J. Electron. Mater. 37 (2008) 288–299.
[9] M. McCormack, S. Jin, G.W. Kammlott, et al., Appl. Phys. Lett. 63 (1993) 15–17.
[10] S. Knott, H. Flandorfer, A. Mikula, Z. Metallkd. 96 (2005) 38–44.
[11] J. Shen, Y.C. Liu, Y.J. Han, et al., J. Electron. Mater. 35 (2006) 1672–1679.
[12] F. Tai, F. Guo, Z.D. Xia, et al., J. Electron. Mater. 34 (2005) 1357–1362.
[13] P. Liu, P. Yao, J. Liu, J. Electron. Mater. 37 (2008) 874–879.
[14] S.M.L. Nai, J. Wei, M. Gupta, J. Electron. Mater. 35 (2006) 1518–1522.
[15] K. Mohan Kumar, V. Kripesh, A. Andrew, et al., J. Alloys Compd. 450 (2008) 229–237.
[16] C. Wei, Y.C. Liu, Y.J. Han, et al., J. Alloys Compd. 464 (2008) 304–305.